

# Enhanced cubic optical nonlinearity of oligoazine derivatives

Vijender Singh · Praveen Aghamkar ·  
Rajesh Kumar Malik

Received: 15 April 2013 / Accepted: 12 August 2013 / Published online: 28 August 2013  
© Springer-Verlag Berlin Heidelberg 2013

**Abstract** We report a large positive third-order optical nonlinearity of synthesized oligoazine derivatives (OADs) using z-scan technique at 532 nm by Q-switched Nd:YAG laser. Optical band gap of OADs shrinks with increasing repeated units. Origin of large cubic nonlinearity is in the extensive  $\pi$ -electron delocalization. We obtained the values of  $\chi_R^{(3)} \approx (0.78 - 3.98) \times 10^{-11}$  esu and  $\chi_I^{(3)} \approx (0.21 - 1.95) \times 10^{-11}$  esu in OADs. Moreover, values of optical nonlinearity of OADs show reasonable agreement with the theoretically predicted values. We have shown OADs could be used as good reverse saturable absorber and self-focusing materials. Optical limiting, due to reverse saturable absorption, has also been successfully demonstrated at 532 nm.

## 1 Introduction

Third-order nonlinear optical (NLO) materials with large optical nonlinearity are needed for numerous optoelectronic device applications including self-focusing, optical limiting, optical switching, and data storage [1–7]. A wide

variety of optical materials have been investigated to obtain a large and tailored optical nonlinearity for matching the requirements of efficient NLO devices [8, 9]. There is a great deal of interest in developing organic materials for NLO devices because these materials have advantages of synthetic flexibility, high damage resistance, and large optical nonlinearities [10]. In particular, conjugated polymers have attracted imperative attention for designing NLO devices as they show extended  $\pi$ -electron delocalization along the chain length and electron-donating/accepting character [8]. In the recent past, third-order NLO property of conjugated systems like polythiophenes, polyacetylenes, polyenes etc. were investigated, and their cubic optical nonlinearity found to be  $10^{-12}$ – $10^{-13}$  esu [11, 12]. Oligoazine is a  $\pi$ -electron conjugate system having an alternate pair of carbon and nitrogen atoms and electron-donating amino group at terminals. The presence of pair of nitrogen atoms in oligoazine derivatives (OADs) provides increased stability toward oxidation and hydrolysis so that materials are environmentally stable. In addition, nitrogen atoms in OADs lead to a wide variety of possible structure modification and also act as electronic perturbation [13]. These properties stimulated our interest to synthesize and investigate third-order NLO properties of OADs and demonstrate their possible functional applications for optoelectronic/photonic. Various techniques have been deployed to study the third-order NLO properties of conjugated system, but each technique has its own merit and demerit, and therefore, they occupy a special place in nonlinear optics [8, 9]. Among them, z-scan technique [14] has a great advantage because of its simplicity and high sensitivity by which one can investigate nonlinear absorption and refraction via open- and closed-aperture measurements, respectively. In addition, signature of nonlinear refractive index can also be deduced.

---

V. Singh  
Department of Applied Science, N.C. College of Engineering,  
Israna, Panipat 132107, Haryana, India

P. Aghamkar (✉)  
Department of Physics, Chaudhary Devi Lal University,  
Sirsa 125055, Haryana, India  
e-mail: p\_ghamkar@yahoo.in

R. K. Malik  
Department of Electronics and Communication Engineering,  
N.C. College of Engineering, Israna, Panipat 132107,  
Haryana, India

In the present work, optical nonlinearity of OADs has been investigated by *z*-scan technique and obtained a large cubic optical nonlinearity. We found an enhancement in optical nonlinearity of OADs occurs due to increase in extensive  $\pi$ -electron delocalization along the chain and electron-donating amino group with increasing sequence of repeated units. To the best of author's knowledge, the study of NLO response of OADs is first time reported by using *z*-scan technique. Results suggest that reverse saturable absorption (RSA) is a responsible mechanism for nonlinear absorption and also optical limiting in OADs, while positive nonlinear refractive index having origin in electronic response leads to self-focusing of optical beam. We found among OADs, heptamer (repeat unit = 7) is one of the most promising candidate materials for optical limiting and self-focusing at 532 nm.

## 2 Experimental

### 2.1 Materials

Yellow powder samples of methyl-substituted oligoazines ( $\text{H}_2\text{N}-[\text{N}=\text{C}(\text{CH}_3)-\text{C}(\text{CH}_3)=\text{N}]_n-\text{NH}_2$ ) with repeat unit = 2, 3, 5, and 7 (also known as dimer, trimer, pentamer and heptamer) were synthesized by chemical route described elsewhere [13]. 2, 3-butanedione (97 %), hydrazine hydrate (AR grade), and glacial acetic acid (99.9 %) were purchased from Sigma-Aldrich and used as received. Solvents like ethanol, tetrahydrofuran (THF), and ether were of analytic grade which are also purchased from Sigma-Aldrich and used without further purification. The synthesis scheme of OADs is illustrated in Fig. 1.

Elemental analysis of yellow powder (as prepared) samples was performed by Perkin-Elmer 2400 CHN elemental analyzer to identify elements. As-prepared samples were also analyzed by  $^1\text{H}$  and  $^{13}\text{C}$  NMR spectroscopy recorded by 400 MHz Bruker (Avance-II) FT NMR spectrophotometer. Fourier transform infrared (FTIR) spectra of the samples were recorded on a Perkin-Elmer spectrophotometer in KBr disks. Also, the ultraviolet visible (UV-VIS) spectra of samples were recorded using a dual beam UV-VIS spectrophotometer (Shimadzu 2550).

### 2.2 Z-scan experiment

In order to study the NLO properties of OADs, single beam *z*-scan technique [14] was used because this technique allows for simultaneous measurement of nonlinear refraction and nonlinear absorption of the materials. Figure 2 shows schematic sketch of the experimental setup for measurement of third-order NLO parameters. The experiment was performed using a Q-switched

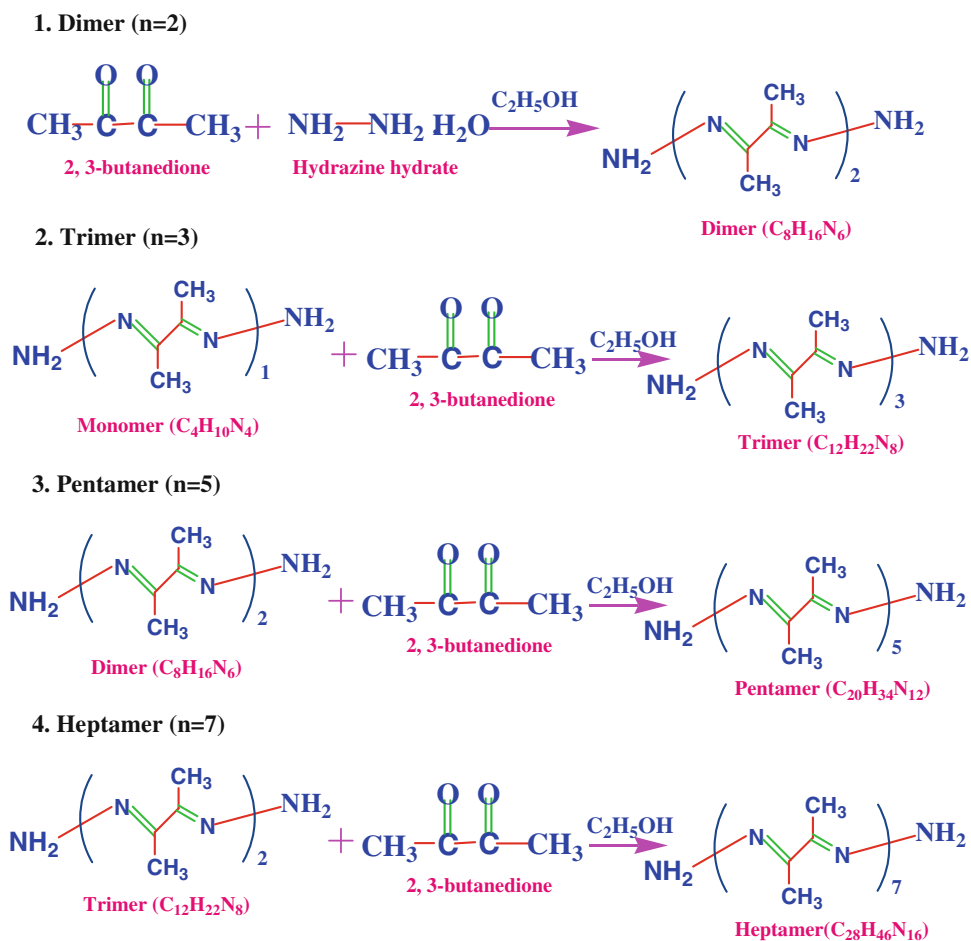
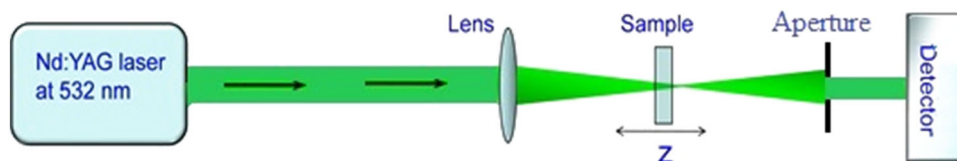
frequency doubled Nd:YAG laser (Quanta system, HYL-101) having a 5 nsec pulse at 532 nm with pulse repetition rate of 10 Hz. The Gaussian laser beam (verified by knife-edge experiment) was tightly focused to a 19.4- $\mu\text{m}$  spot. First of all, the *z*-scan experimental setup was calibrated with  $\text{CS}_2$  to measure third-order nonlinear absorption and refraction coefficients of powder OADs dissolved in THF ( $\approx 1$  mM concentration) and was kept in a quartz cell (sample holder) of 1.0-mm path length (*l*). Thin sample approximation, i.e.,  $l < z_0$  ( $z_0 = \pi w_0^2/\lambda$  is the Rayleigh range, where  $w_0$  is the spot size of the beam) for all the samples was ensured. The samples were mounted on a xyz translation stage (THORLABS-PT-3-1), and it was translated along the *z*-axis with respect to the focal point. The transmitted pulse energy was collected by a detector (Thorlab DET 110) and was analyzed by 200-MHz digital storage oscilloscope (Tektronix TDS 2024). In this work, intensity of the laser was kept  $\approx 0.2$  GW/cm<sup>2</sup>, and we noticed that scattering and thermal effects were very weak at this intensity and hence neglected them without losing the generality of the problem [15]. Moreover, low repetition rate of the laser allows one to neglect the contribution of pulse-to-pulse build-up effect [16]. For optical power limiting study, the samples in quartz cuvette were placed just behind the focus of the laser beam. By varying the input energy, the change in the output of the laser energy was recorded using DigiRad (R-752) universal radiometer.

## 3 Results and discussion

### 3.1 Characterizations

The elemental analysis data (see Table 1) shows that the percentage of carbon in OADs gradually increases as their number of repeated units (i.e., chain length) increases. In Table 1  $^1\text{H}$  and  $^{13}\text{C}$  NMR, data is also given, where its spectra are shown in Figs. 3 and 4, respectively. In  $^1\text{H}$  spectra, peak at 1.805 ( $\pm 0.015$ ) ppm is due to methyl groups attached to imine carbons in OADs chain, while a peak due to amino proton was found in range 5.50–5.55 ppm. The more extensive conjugation of the oligoazine  $\pi$ -system leads to increased deshielding of protons so that the observed resonances are all downfield of the corresponding chemical shift of the dimer resonance. The  $^{13}\text{C}$  NMR spectra of OADs show strong resonances in the two different range: near 8.0–15.5 ppm, attributed to the methyl carbons and near 149.0–165.5 ppm, due to imine carbons.

The FTIR spectra of the prepared OADs recorded in the range 400–4,000  $\text{cm}^{-1}$  are shown in Fig. 5. It is pertinent to mention here that the spectra of OADs resemble with its

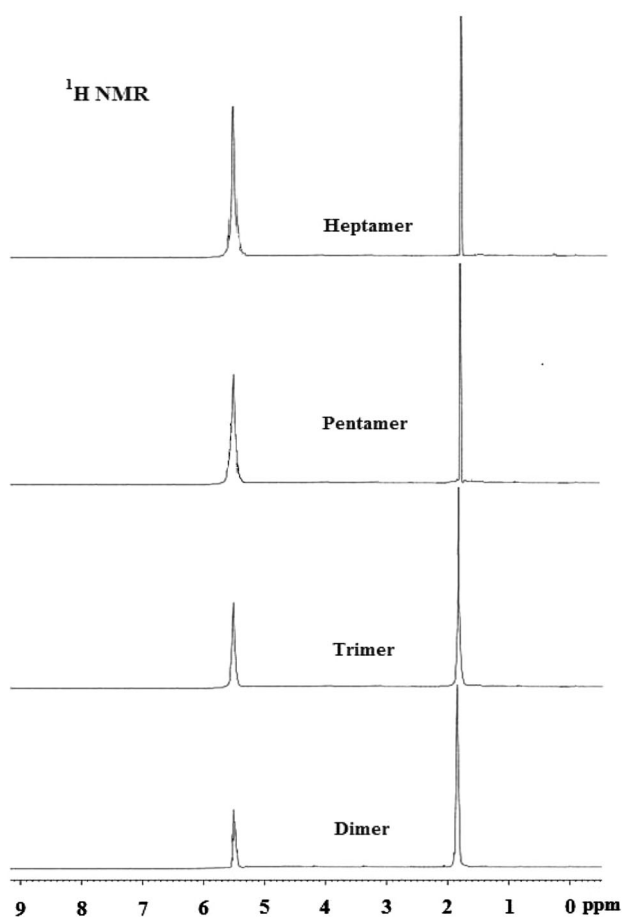
**Fig. 1** Synthesis scheme of OADs**Fig. 2** Z-scan experimental setup

monomer spectrum reported elsewhere [5]. Various absorption bands/peaks are described as follows:  $\nu$  (asymmetric stretch NH<sub>2</sub>) 3,340 cm<sup>-1</sup>,  $\nu$  (symmetric stretch NH<sub>2</sub>) 3,290 cm<sup>-1</sup>,  $\nu$  (symmetric stretch C–H) 2,930 cm<sup>-1</sup>,  $\nu$  (internal deformation NH<sub>2</sub>) 1,615–1,620 cm<sup>-1</sup>,  $\nu$  (C=N stretching) 1,570 cm<sup>-1</sup>,  $\nu$  (asymmetric deformation C–CH<sub>3</sub>) 1,470–1,475 cm<sup>-1</sup>,  $\nu$  (C–CH<sub>3</sub> stretching) 1,375 cm<sup>-1</sup>,  $\nu$  (N–N stretching) 1,110 cm<sup>-1</sup>, and  $\nu$  (N–H rocking) 690–715 cm<sup>-1</sup>. Some peaks between 950 and 1,100 cm<sup>-1</sup> are unassigned but are probably associated with single vibration along the molecular backbone [13]. FTIR results support NMR data of OADs. To this end, we discussed the percentage of carbon, hydrogen, and nitrogen and how it influences delocalization of  $\pi$ -electron in backbone. Further, it was confirmed by FTIR data.

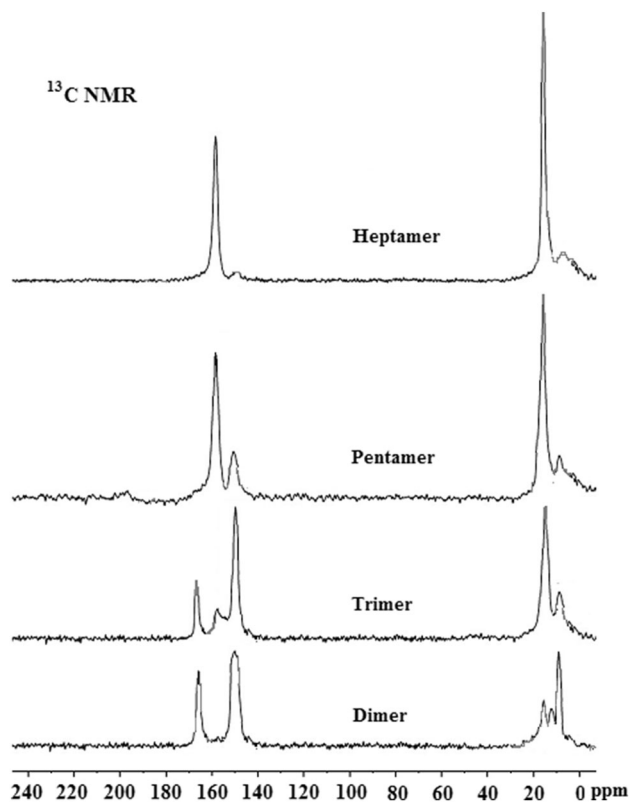
The z-scan technique mainly depends on absorption spectra of the samples. The linear absorption spectra of OAs are shown in Fig. 6 in which absorption bands (around 280 and 300 nm) attribute to  $\pi \rightarrow \pi^*$  transition. This transition leads to strong charge transfer in OADs [18]. It is also noticed that OADs exhibit hyperchromic and bathochromic effects with increasing chain length. Furthermore, assuming OADs as direct band-gap materials, their optical band gap ( $E_g$ ) are extracted from linear absorption coefficient ( $\alpha$ ) by using well-known Tauc relation [19]. Figure 7 shows  $h\nu$  versus  $(\alpha h\nu)^2$  plot for all the samples. This plot depicts a gradual decrease in  $E_g$  as number of repeated units increases. This characteristic of OADs makes them promising optical materials for obtaining a large and tailored third-order nonlinearity ( $\chi^{(3)}$ ) because  $\chi^{(3)} \propto E_g^{-6}$

**Table 1** Elemental,  $^1\text{H}$  NMR and  $^{13}\text{C}$  NMR data of OADs

| Samples         | Elemental analysis        |      |       | Major peaks      |                        |
|-----------------|---------------------------|------|-------|------------------|------------------------|
|                 | Percentage of C, H, and N |      |       | $^1\text{H}$ NMR | $^{13}\text{C}$ NMR    |
|                 | C                         | H    | N     |                  |                        |
| <b>Dimer</b>    |                           |      |       |                  |                        |
| Calc.           | 48.94                     | 8.20 | 42.86 | 1.82 (3H)        | 9.5, 12.0 and 15.5     |
| Found           | 48.82                     | 8.12 | 42.96 | 5.52 (2H)        | 149.5 and 165.0        |
| <b>Trimer</b>   |                           |      |       |                  |                        |
| Calc.           | 51.78                     | 7.98 | 40.25 | 1.81 (3H)        | 9.0 and 15.0           |
| Found           | 51.69                     | 8.0  | 40.17 | 5.50 (2H)        | 149.5, 158.5 and 165.5 |
| <b>Pentamer</b> |                           |      |       |                  |                        |
| Calc.           | 54.27                     | 7.73 | 38.0  | 1.80 (3H)        | 9.0 and 15.5           |
| Found           | 54.35                     | 7.62 | 37.85 | 5.50 (2H)        | 150.0 and 159.0        |
| <b>Heptamer</b> |                           |      |       |                  |                        |
| Calc.           | 55.40                     | 7.65 | 36.94 | 1.79 (3H)        | 8.0 and 15.5           |
| Found           | 55.02                     | 7.57 | 37.9  | 5.55 (2H)        | 149.0 and 160          |

**Fig. 3**  $^1\text{H}$  NMR spectra of OADs

[20]. In particular, ( $E_g$ ) of heptamer is nearly 0.94 smaller than that of dimer ( $R_u = 2$ ), and as results ( $\chi^{(3)}$ )<sub>heptamer</sub> becomes larger than the ( $\chi^{(3)}$ )<sub>dimer</sub>. This result suggests that

**Fig. 4**  $^{13}\text{C}$  NMR spectra of OADs

optical response of OADs can be tailored through their synthesis flexibility for future molecular engineering.

### 3.2 Z-scan

An open-aperture transmission of all the samples was measured in the far field to find out their respective

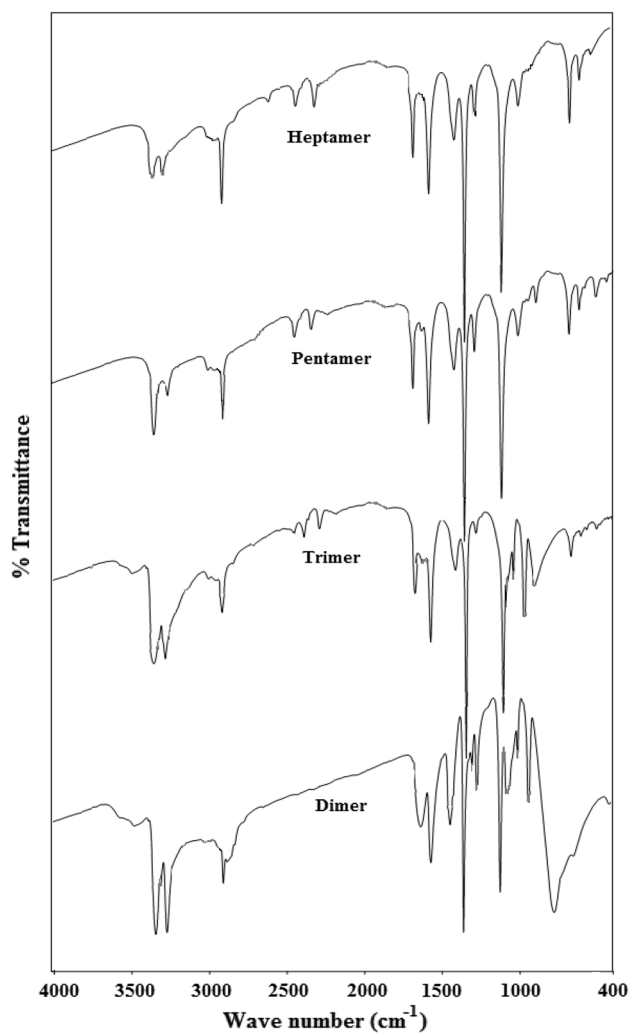


Fig. 5 FTIR spectra of OADs

nonlinear absorption coefficients. Figure 8 shows a decrease in transmittance around the focal point of all the scanned samples, which is indicative of nonlinear absorption in OADs. In this figure, symbols represent experimental transmission data, while solid lines are obtained by fitting the experimental data to the nonlinear transmittance given by relation [14]  $T(z, S = 1) = \sum_{m=0}^{\infty} \frac{[-q_0(z)]^m}{(m+1)^{3/2}}$  for  $q_0(z) < 1$ ; with  $q_0(z) = \frac{\beta I_0 L_{\text{eff}}}{(1+z^2/z_0^2)}$ , and  $L_{\text{eff}} = [1 - \exp(-\alpha l)]/\alpha$ . Here  $z$  is the sample position, while  $\beta$ ,  $I_0$ , and  $L_{\text{eff}}$  are the nonlinear absorption coefficient, intensity of light at the focus, and effective length of the sample, respectively. Open-aperture experimental data of OADs are found fit well for typical values of  $\beta$  and their corresponding imaginary part of third-order susceptibilities ( $\text{Im}\chi^{(3)}$ ) are also evaluated (see Table 2). Nonlinear absorption coefficient may include instantaneous two-photon-type absorption and excited-state absorption (ESA)/reverse saturable absorption (RSA). In general, in each of the wavelength

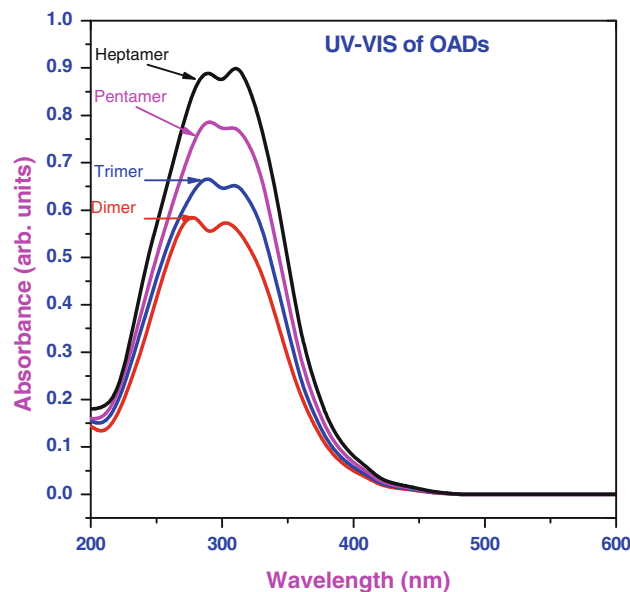
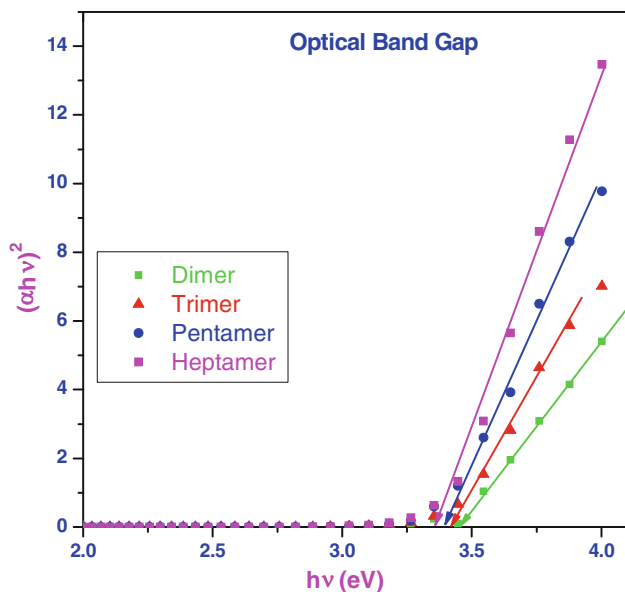


Fig. 6 Optical absorption spectra of OADs

region, the nonlinear absorption of the materials depends mainly on the laser–matter interaction time and cross-section area of excited states. The nonlinear absorption observed in OADs can be explained by using a five-level model [21] involving the states including singlet states ( $S_1$  and  $S_2$ ) and triplet states ( $T_1$  and  $T_2$ ), and every electronic energy level involves several vibronic levels as shown in Fig. 9. On interaction with a 5-ns laser pulse at 532 nm, OADs get excited from the  $S_0$  to upper vibrational levels of  $S_1$  via instantaneous two-photon-type absorption. Through nonradiative decay within picosecond time scale, the excited molecules can relax to the lowest vibrational level of  $S_1$ . We consider  $S_1$ – $S_2$  transition does not deplete the  $S_1$  state because the  $S_1$ – $S_2$  transition takes place in much shorter time than the pulse duration. From  $S_1$ , electrons are transferred to  $T_1$  via intersystem crossing and subsequently transition  $T_1$ – $T_2$  (triplet–triplet absorption) occurs. With excitation of laser pulse on the nanosecond scale, which is true in our case, triplet–triplet excited-state absorption (ESA) is expected to make significant contribution to nonlinear absorption. Furthermore, Fig. 8 depicts normalized transmittance minima occurring around the focal plane, which infer ESA turns to RSA character in all the samples [21]. This feature has been confirmed by comparing magnitude of cross section of the ground state ( $\sigma_{S_0}$ ) and cross section of first triplet excited state ( $\sigma_{T_1}$ ) of the sample. Following Henari et al. approach [20], numerical value of ( $\sigma_{S_0}$ ) and ( $\sigma_{T_1}$ ) were obtained (See Table 2) and found that  $\sigma_{T_1} > \sigma_{S_0}$  in all the samples, which confirms RSA is responsible mechanism for nonlinear absorption in OADs.

Now, we focus our study on signature and magnitude of nonlinear refractive index ( $n_2$ ) of OADs. For this purpose, a



**Fig. 7** Optical band gap of OADs

closed-aperture measurements of z-scan were performed for all the samples, and normalized transmittance (symbols) are shown in Fig. 10, wherein the solid lines are obtained by fitting relation  $T(x, \Delta\phi_0) = 1 + \frac{4|\Delta\phi_0|x}{[x^2+1][x^2+9]}$  with  $x = z/z_0$  and  $|\Delta\phi_0| = (2\pi/\lambda)(n_2)_{\text{exp}t}I_0L_{\text{eff}}$  is the phase change. The value of  $|\Delta\phi_0|$  is calculated from the peak-valley transmittance difference ( $\Delta T_{\text{P-V}}$ ) using equation [14], for  $\Delta T_{\text{P-V}} = 0.406(1 - S)^{0.25}|\Delta\phi_0|$ ,  $|\Delta\phi_0| \leq \pi$ , where  $S$  is the linear transmittance of a far-field aperture ( $S = 0.39$  in this work). We fitted our closed-aperture data to the theoretical model [14], which provides excellent agreement for typical values of  $(n_2)_{\text{exp}t}$  and also obtained corresponding real part of third-order optical susceptibilities ( $\text{Re}\chi^{(3)}$ ) (See Table 2). It is clearly evident from Fig. 10 that all the samples exhibit prefocal valley and post-focal peak characteristics, which is a direct indication of positive nonlinear refractive index (positive lens), and it suggests OADs can also be used as a good self-focusing materials around 532 nm. The observed refractive nonlinearity is electronic in origin because in OADs, amino group donates electron which respond almost freely to an applied optical field [14, 22]. Moreover, peak-valley character of OADs satisfies the condition of  $\Delta Z_{\text{P-V}} \sim 1.7z_0$  (Where,  $\Delta Z_{\text{P-V}}$  is the separation between the maxima and minima of the closed-aperture curves), thus confirming the refractive nonlinearity is due to electronic process [14]. In order to test experimentally obtained values of nonlinear refractive index of samples, we have used well-known Boling-Glass-Owyong (BGO) empirical formula [23]:  $(n_2)_{\text{calc}} = \frac{(gf)(n_0^2+2)^2(n_0^2-1)^2}{48\pi n_0 \hbar \omega_0 (Nf)}$  (where  $n_0$ ,  $f$ , and  $N$  are background refractive index, oscillator strength, and density of

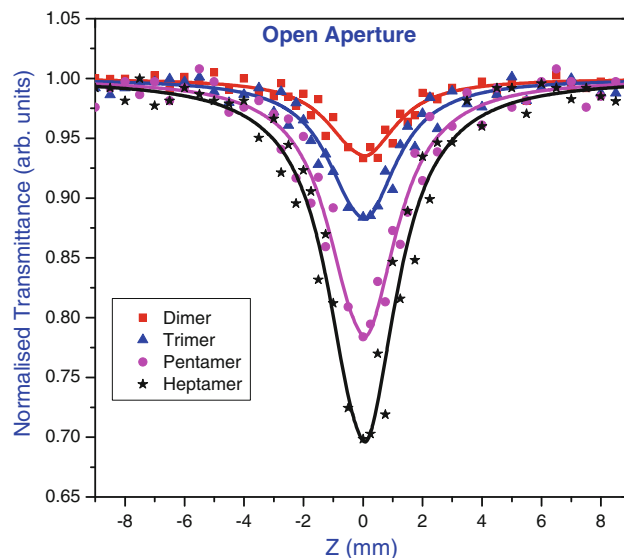


**Fig. 8** Open-aperture measurements (at 532 nm) of OADs. Solid curve represents theoretical fits

molecules in units of  $\text{mol}/\text{cm}^3$ , respectively, while  $(gf)$  is the free parameter set equal to 3). The calculated and experimental values of nonlinear refractive index are given in Table 2. Here, we assumed, dispersion behavior of linear polarizability ( $\alpha_l$ ), and nonlinear refractive index of OADs are similar in nature under the consideration of off-resonant transition regime (i.e.,  $E_g < \hbar\omega_0$ ). This assumption allows one to consider origin of  $n_2$  solely in electronic effect and neglect contribution of nuclear motion or reorientation effects.

One of the necessary steps in improving the NLO properties of conjugated polymers is to gain a basic understanding of the relationship that exists between third-order nonlinearity and second hyperpolarizability  $\gamma[\chi^{(3)} \propto \gamma]$ . The second hyperpolarizability ( $\gamma$ ) describes the nonlinear induced electronic polarization per molecule [24], which is related to  $(n_2)_{\text{exp}t}$  as:  $\gamma_{\text{exp}t} = \frac{4(n_2)_{\text{exp}t}n_0^2\epsilon_0c}{3L^4N}$ , where  $L$  is the local field factor which in the Lorentz approximation is given by  $L = (n_0^2 + 2)/3$ . While calculated values of second hyperpolarizability ( $\gamma_{\text{calc}}$ ) are obtained by relation  $\gamma_{\text{calc}} = \frac{g\alpha_l^2}{\hbar\omega_0}$  (here,  $g$  is the free parameter). Computed values of  $\gamma_{\text{exp}t}$  and  $\gamma_{\text{calc}}$  are summarized in Table 2. In this table, one may notice that measured values show reasonable agreement with the theoretically predicted values for dimer and trimer, while agreement is deprived for the case of pentamer and heptamer. This is because as the number of repeated units increases, on one hand,  $n_2$  and  $\gamma$  varies significantly, and on the other hand, solubility problem arises [25]. Moreover, the BGO empirical formula was obtained by considering several assumptions [23] and was found to predict  $n_2$  within an average accuracy of



**Table 2** Optical band gap, excited and ground state cross sections, NLO coefficients (measured and calculated) of OADs

| Samples  | $E_g$ (eV) | $\sigma_{T_1}$ ( $10^{-20}$ cm <sup>2</sup> ) | $\sigma_{S_0}$ ( $10^{-21}$ cm <sup>2</sup> ) | $\beta$ (cm/GW) | $\chi_I^{(3)}$ ( $10^{-11}$ esu) | $(n_2)_{exp, r}$ ( $10^{-13}$ cm <sup>2</sup> /W) | $(n_2)_{calc}$ ( $10^{-13}$ cm <sup>2</sup> /W) | $\chi_R^{(3)}$ ( $10^{-11}$ esu) | $\chi^{(3)}$ ( $10^{-11}$ esu) | $\gamma^{exp, r}$ ( $10^{-30}$ esu) | $\gamma^{calc}$ ( $10^{-30}$ esu) |
|----------|------------|---|---|-----------------|----------------------------------|---|---|----------------------------------|--------------------------------|-------------------------------------|-----------------------------------|
| Dimer    | 3.48       | 0.58  | 0.88  | $0.1 \pm 0.01$  | $0.21 \pm 0.02$                  | $1.58 \pm 0.18$                                   | 0.97  | $0.78 \pm 0.09$                  | $0.81 \pm 0.09$                | $1.08 \pm 0.12$                     | 0.63                              |
| Trimer   | 3.47       | 1.30  | 2.05  | $0.22 \pm 0.02$ | $0.46 \pm 0.05$                  | $2.63 \pm 0.31$                                   | 1.97  | $1.31 \pm 0.15$                  | $1.39 \pm 0.16$                | $4.17 \pm 0.5$                      | 2.94                              |
| Pentamer | 3.46       | 2.92  | 3.21  | $0.48 \pm 0.05$ | $1.02 \pm 0.01$                  | $4.26 \pm 0.51$                                   | 2.98  | $2.12 \pm 0.25$                  | $2.35 \pm 0.28$                | $10.5 \pm 1.2$                      | 6.96                              |
| Heptamer | 3.45       | 5.55  | 10.1  | $0.92 \pm 0.1$  | $1.95 \pm 0.23$                  | $8.02 \pm 0.96$                                   | 3.01  | $3.98 \pm 0.47$                  | $4.44 \pm 0.53$                | $62.32 \pm 7.4$                     | 29.4                              |

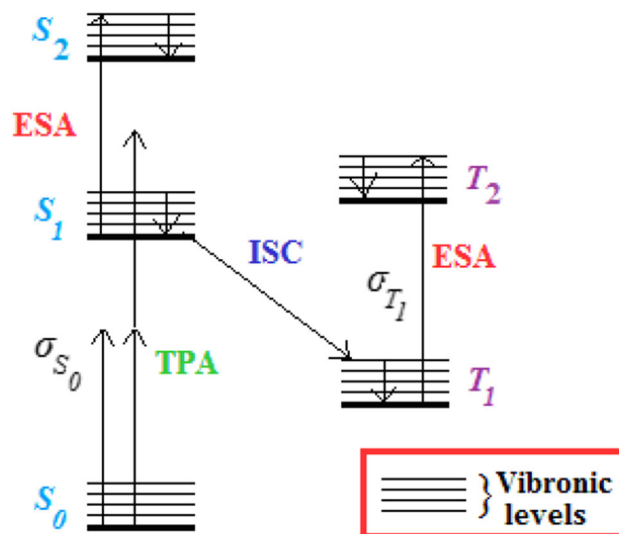


**Fig. 9** Schematic diagram of five-level energy model

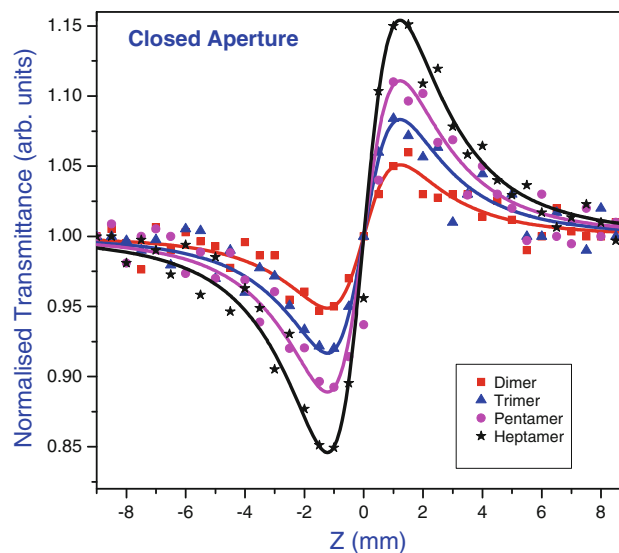


**Fig. 10** Closed-aperture measurements (at 532 nm) of OADs. *Solid curve* represents theoretical fits

about 30 % for a variety of types of crystal [26]. It is expected that a better match between experiment and theory could be obtained by measurement of the transmittance (open and closed aperture) as a function of intensity for OADs. This study will be subject of future communication.

The investigation of cubic nonlinearity of OADs suggest that triplet–triplet transition (RSA) is sole mechanism for nonlinear absorption, while nonlinear refraction having origin in electronic response leads to self-focusing of optical beam. Generally, in  $\pi$ -conjugated oligomers/polymers, the charge cloud formed by conjugated  $\pi$ -electrons has the capability of being strongly deformed under the effect of an external optical field [12]. The electron moves

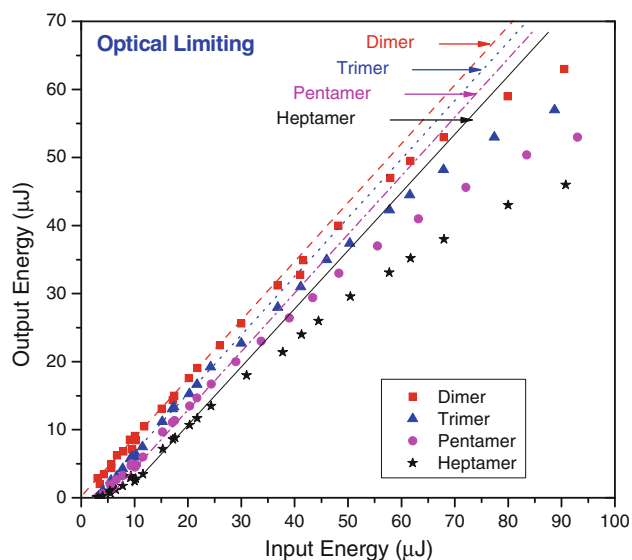


**Fig. 11** Optical limiting behavior of OADs

in large molecular orbitals, formed by the linear superposition of carbon  $P_z$  atomic orbitals, which results in enhancement of  $\chi^{(3)}$  with increasing repeated units. Interestingly, reported values (summarized in Table 2) are larger than the values measured in OADs using third harmonic generation technique [27] and quoted for different conjugated polymers like polyenes [28], thiophene, oligomers [25], and polyazine monomer [5] under similar experimental conditions. Z-scan measurements were also demonstrated separately for an empty quartz cell and pure THF with aforesaid experimental conditions. It was noticed that nonlinear absorption and refraction of empty quartz cell and pure THF were found negligible, and hence, study of nonlinear absorption and refraction of the solution attribute to only OADs. The expected errors (obtained from experimental and fitting procedure) in these measurements were estimated to be around 12%. The main source of errors in the experimental data arose from: (1) uncertainty in determining the focused spot size (and therefore, the intensity at the sample) from the measured divergence, (2) Rayleigh range and absorbance, (3) laser power fluctuations, and (4) uncertainty in the fitting procedure.

An ultimate practical goal for designing OADs with a large cubic nonlinearity is to incorporate them into optoelectronic and photonic devices, and hence, possibility of optical limiting and optical switching in OADs were examined around 532 nm by using a nanosecond pulse laser. For optical limiting, the measurements were performed in open-aperture configuration and are plotted in Fig. 11. In this plot, straight lines represent linear transmittance in the absence of nonlinear absorption contribution. Nonlinear absorption in all samples

enhances with increase in input energy, due to enhancement of triplet–triplet absorption (RSA), which results in a deviation from their linear transmittance. It is also noticed that OADs having more number of repeated units block the incident light more effectively at higher incident energy than the OADs having less number of repeated units (see Fig. 11). Among OADs, heptamer show largest absorption cross-section area ( $\sigma_{T_1}$ ), and therefore, it is one of the most promising candidate materials for RSA around 532 nm and hence for optical limiting also. Furthermore, the possibility of optical switching is also examined via figure of merit ( $FOM = \beta\lambda/(n_2)_{\text{exp}}$ ) [29] and found that FOM ranges 3.47–6.15. This result suggests that contribution of nonlinear absorption dominates over nonlinear refraction, which impedes good optical switching behavior.

## 4 Conclusions

In summary, OADs were synthesized by chemical route, and the percentage of content of as-prepared samples was analyzed. Also, the as-prepared samples were characterized by  $^1\text{H}$  and  $^{13}\text{C}$  NMR and FTIR spectroscopy. Linear and third-order NLO properties of OADs were determined. We found that optical band-gap shrinks as more repeated units are introduced into the oligoazine backbone and leads to lengthen its  $\pi$ -conjugation. The third-order NLO absorption and refraction coefficients and also second hyperpolarizability of OADs have been obtained by z-scan technique with frequency doubled, Q-switched 5 nsec Nd:YAG laser at wavelength 532 nm. The dependence of NLO coefficients on number of repeated units have been investigated, and it is found that magnitude of NLO coefficient increases with increasing number of repeated units. This result indicates that optical nonlinearities of conjugated system may synthetically tailored by varying length of conjugated  $\pi$ -systems and by evaluating the effects of their electron-donating groups. Measured values of optical nonlinearity of OADs show reasonable agreement with the theoretically predicted values. We found RSA is a responsible mechanism for nonlinear absorption and optical limiting in OADs at 532 nm. In addition, the signature of nonlinear refractive index in OADs is positive, and hence, these derivatives could be used as good self-focusing materials. OADs investigated here are possible promising candidate optical materials for the development of optoelectronic and photonic devices like self-focusing and optical limiting at 532 nm. Further extension of this work to study the effect of intensity on OADs in nano- and picosecond time scale shall be the subject of future communication.



**Acknowledgments** This work was supported by AICTE (RPS scheme), New Delhi, for providing financial support.

## References

1. Y.H. Lee, Y. Yan, L. Polavarapu, Qing-Huaxu, *Appl. Phys. Lett.* **95**, 023105 (2009)
2. M. Feng, H. Zhan, Y. Chen, *Appl. Phys. Lett.* **96**, 033107 (2010)
3. M. Singh, P. Aghamkar, *Opt. Commun.* **281**, 1251 (2008)
4. P. Aghamkar, M. Singh, *J. Mod. Opt.* **56**, 931 (2008)
5. V. Singh, P. Aghamkar, *Appl. Opt.* **51**, 2288 (2012)
6. X. Wang, S. Guang, H. Xu, X. Yang, Y. Song, N. Lin, X. Liu, *J. Mat. Chem.* **18**, 4204 (2008)
7. S.M. O' Flaherty, S.V. Hold, M.E. Brennan, M. Cadec, A. Drury, J.N. Coleman, W.J. Blau, *J. Opt. Soc. Am. B* **20**, 49 (2003)
8. H.S. Nalwa, S. Miyata, *Nonlinear optics of organic molecules and polymers* (CRC press, Boca Raton, 1997)
9. R.L. Sutherlands, *Handbook of nonlinear optics* (Marcel Dekker, New York, 2003)
10. B. Gu, W. Ji, P.S. Patil, S.M. Dharmarkash, *J. Appl. Phys.* **103**, 103511 (2008)
11. H.S. Nalwa, *Nonlinear optical properties of  $\pi$ -conjugated materials: in Handbook of organic conductive molecules and polymers*, vol. 4 (Wiley, U.S., 1997)
12. P. Poornesh, G. Umesh, P.K. Hegde, M.G. Manjunatha, K.B. Man, A.V. Adhikari, *Appl. Phys. B* **97**, 117 (2009)
13. C.R. Hauer, G.S. King, E.L. McCool, W.B. Euler, J.D. Ferrara, W.J. Youngs, *J. Am. Chem. Soc.* **109**, 5760 (1987)
14. M. Sheik Bahae, E.W. Van Stryland, *IEEE J. Quant. Elect.* **26**, 760 (1990)
15. F. Li, Y. Song, K. Yang, S. Liu, C. Li, *Appl. Phys. Lett.* **71**, 2073 (1997)
16. S. Yamada, H. Matsuda, D. Yankelevich, S. Yamada, H. Matsuda, *Appl. Phys. Lett.* **72**, 1021 (1998)
17. W.B. Euler, J.E. Roberts, *Macromolecules* **22**, 4221 (1989)
18. B.C. Sherman, B.K. Schmitz, W.B. Wuler, *Chem. Mater.* **7**, 806 (1995)
19. J. Tauc, A. Menth, *J. Non-Cryst. Solids* **8**, 569 (1972)
20. G.P. Agarwal, C. Flytzanis, *Chem. Phys. Lett.* **44**, 366 (1976)
21. F.Z. Henari, *J. Opt. A Pure Appl. Opt.* **3**, 188 (2001)
22. K. Iliopoulos, R. Czaplinski, H.E. Ouazzani, J.Y. Balandier, M. Chas, *Appl. Phys. Lett.* **97**, 101104 (2010)
23. N.L. Boling, A.J. Glass, A. Owyong, *IEEE J. Quantum Electron.* **14**, 601 (1978)
24. R.W. Boyd, *Nonlinear Optics* (Academic press, USA, 2008)
25. M.-T. Zhao, B.P. Singh, P.N. Prasad, *J. Chem. Phys.* **89**, 5535 (1988)
26. R. Adair, L.L. Chase, S.A. Payne, *Phys. Rev. B* **39**, 3337 (1989)
27. H.S. Nalwa, T. Hamada, A. Kakuta, A. Mukoh, *Synth. Met.* **57**, 3901 (1993)
28. R.C. Beltran, G.O. Ramos, C.K.W. Jim, J.L. Maldonado, M. Haubler, D.P. Dominguez, *Appl. Phys. B* **97**, 489 (2009)
29. T. Huang, Z. Hao, H. Gong, Z. Liu, S. Xiao, S. Li, *Chem. Phys. Lett.* **451**, 213 (2008)